NeuroImage 202 (2019) 116050

Contents lists available at ScienceDirect

NeuroImage

journal homepage: www.elsevier.com/locate/neuroimage

Sensorimotor cortex neurometabolite levels as correlate of motor performance in normal aging: evidence from a ^{1}H-MRS study

Oron Levin [a,*,‡], Akila Weerasekera [b,‡], Bradley R. King [a], Kirstin F. Heise [a], Diana M. Sima [c], Sima Chalavi [a], Celine Maes [a], Ronald Peeters [d], Stefan Sunaert [d], Koen Cuypers [a,e], Sabine Van Huffel [f], Dante Mantini [a,g], Uwe Himmelreich [b,1], Stephan P. Swinnen [a,h,1]

[a] Movement Control & Neuroplasticity Research Group, Department of Movement Sciences, Group Biomedical Sciences, KU Leuven, Belgium
[b] Biomedical MRI Unit, Department of Imaging & Pathology, Group Biomedical Sciences, KU Leuven, Belgium
[c] Icometrix, R&D, Leuven, Belgium
[d] Department of Radiology, University Hospitals Leuven, UZ Gasthuisberg, Belgium
[e] REVAL Research Institute, Hasselt University, Agoralaan, Building A, B-3590, Diepenbeek, Belgium
[f] Department of Electrical Engineering (ESAT), STADIUS Centre for Dynamical Systems, Signal Processing and Data Analytics, KU Leuven, Belgium
[g] Brain Imaging and Neural Dynamics Research Group, IRCCS San Camillo Hospital, Venice, Italy
[h] KU Leuven, Leuven Brain Institute (LBI), Leuven, Belgium

ARTICLE INFO

Keywords:
Aging
Coordination
Magnetic resonance spectroscopy
Motor control
Neurometabolites

ABSTRACT

Aging is associated with gradual alterations in the neurochemical characteristics of the brain, which can be assessed in-vivo with proton-magnetic resonance spectroscopy (^{1}H-MRS). However, the impact of these age-related neurochemical changes on functional motor behavior is still poorly understood. Here, we address this knowledge gap and specifically focus on the neurochemical integrity of the left sensorimotor cortex (SM1) and the occipital lobe (OCC), as both regions are main nodes of the visuomotor network underlying bimanual control. ^{1}H-MRS data and performance on a set of bimanual tasks were collected from a lifespan (20–75 years) sample of 86 healthy adults. Results indicated that aging was accompanied by decreased levels of N-acetylaspartate (NAA), glutamate-glutamine (Glx), creatine + phosphocreatine (Cr) and myo-inositol (mI) in both regions, and decreased Choline (Cho) in the OCC region. Lower NAA and Glx levels in the SM1 and lower NAA levels in the OCC were related to poorer performance on a visuomotor bimanual coordination task, suggesting that NAA could serve as a potential biomarker for the integrity of the motor system supporting bimanual control. In addition, lower NAA, Glx, and mI levels in the SM1 were found to be correlates of poorer dexterous performance on a bimanual dexterity task. These findings highlight the role for ^{1}H-MRS to study neurochemical correlates of motor performance across the adult lifespan.

1. Introduction

Normal aging is associated with gradual alterations in structural and neurochemical characteristics of the brain, the latter of which can be assessed in-vivo by the application of proton-magnetic resonance spectroscopy (^{1}H-MRS). Changes in the regional levels of N-acetylaspartate (NAA), choline (Cho), myo-inositol (mI), gamma-aminobutyric acid (GABA), and glutamate-glutamine complex (Glx) have been identified as potential biomarkers of disease progression in neurodegenerative disorders and dementia (Ben Salem et al., 2008; Block et al., 1998; Bonneville et al., 2002; Ding et al., 2008; Duarte et al., 2012; Kalra et al., 2006; Kantarci et al., 2007; Weerasekera et al., 2018; Zanigni et al., 2015). In healthy human volunteers, in-vivo quantification of brain neurometabolites with ^{1}H-MRS typically shows age-related declines in regional levels of multiple neurometabolites, including NAA, Glx, creatine + phosphocreatine (Cr), and GABA and increases in the levels of Cho and mI (Boumezbeur et al., 2010; Ding et al., 2016; Gao et al., 2013; Grachev and Apkarian, 2001; Grachev et al., 2001; Haga et al., 2009;

* Corresponding author. Movement Control & Neuroplasticity Research Group, Department of Movement Sciences, KU Leuven, Tervuurse Vest 101, 3001, Leuven, Belgium.
E-mail address: oron.levin@kuleuven.be (O. Levin).
‡ Equal contributions as first author.
1 Equal contributions as last author.

https://doi.org/10.1016/j.neuroimage.2019.116050
Received 30 March 2019; Received in revised form 17 June 2019; Accepted 22 July 2019
Available online 23 July 2019
1053-8119/© 2019 Elsevier Inc. All rights reserved.

Hermans et al., 2018a; Maes et al., 2017; Porges et al., 2017; Valenzuela et al., 2000; Zahr et al., 2013). These alterations may play a pivotal role as mediators of progressive performance declines observed during aging in an apparently healthy population.

Considering that neurochemical alterations could be indicative of neurodegenerative processes at the neuronal network levels, one would expect to find an association between age-related changes in the regional levels of GABA, NAA, Cho, mI, and Glx (among other neurochemicals and/or neurotransmitters) and degraded motor performance (Zahr et al., 2013; Hermans et al., 2018b). However, very little attention has been paid so far to the age-related declines in motor functioning, and in complex motor tasks (e.g., bimanual coordination) in particular. The current study will address this critical knowledge gap by examining the associations between age-related changes in the integrity of neurochemical systems in the left primary sensorimotor (SM1) and occipital (OCC) cortical regions and performance changes across two specific bimanual tasks: a visuomotor bimanual coordination task (BCT) and bimanual Purdue pegboard task (PPT). Both tasks are useful for studying the associations between neurodegenerative changes in the aging brain and performance changes that could be attributed to suboptimal operation of the cortical visuomotor network underlying bimanual coordination (Fujiyama et al., 2016; King et al., 2017; Serbruyns et al., 2015; Sisti et al., 2011). The SM1 and OCC were selected on the basis of previous task-related fMRI studies on bimanual tracking tasks under visual guidance (e.g., Beets et al., 2015; Santos Monteiro et al., 2017), showing that both regions are principal nodes of the sensorimotor system supporting visuomotor control.

In an early study of our group using a variant of the BCT (Fujiyama et al., 2016), we demonstrated that older adults who showed performance declines in more difficult bimanual conditions also showed a decreased ability to regulate the interaction between dorsolateral prefrontal cortex and the primary motor cortex (M1). In line with these findings, we expected that (1) lower Glx levels in the sensorimotor voxel will be related to decreased performance on BCT as both excitatory and inhibitory interactions between M1 and other brain regions are expected to rely primarily on activation of glutamatergic transmission (Chen, 2004; Levin et al., 2014; Liuzzi et al., 2010; Perez and Cohen, 2008). In addition, we expected that (2) age-related performance declines in BCT (and bimanual PPT) will be related to decreases in the level of NAA, which is generally considered to be associated with GM loss (Ding et al., 2016) and WM microstructural declines (Grossman et al., 2015; Wijtenburg et al., 2013) that may hinder bimanual control. Finally, we expected that (3) higher levels of Cho and mI would be related to poorer performance on both tasks, since increased concentrations of these metabolites have been associated with cerebral infarction under various neuropathological conditions or diseases (Soares and Law, 2009). However, there is a certain degree of controversy in the literature regarding the effects of normal healthy aging on mI and Cho concentrations (Cichocka and Bereś, 2018; Cleeland et al., 2019). Therefore, it was not possible to form clear hypotheses about the nature of the relationship between age-related changes in regional concentrations of mI or Cho and performance on the two bimanual tasks.

2. Methods

2.1. Participants

We included 106 healthy, right-handed (Oldfield, 1971) adults (age range 20.0–74.5 years, 49 women) that were from the same pool of participants as in King et al. (2017). All participants had no past or present history of neurological or psychiatric disorders, no contra-indications for magnetic resonance imaging (as indicated in the guidelines of the University Hospital Leuven), normal or corrected to normal vision, and reported no consumption of psychoactive medications at the time of the experiment. The experimental protocol was approved by the local medical ethics committee (University Hospital Leuven; MEC reference S58441), and a written informed consent was obtained from each of the participants prior to his/her inclusion in the study. Fifteen of the 106 participants were excluded from the final analyses due to missing data and/or poor quality of MRI/MRS acquisition. Two participants voluntarily withdrew from the study before completion of the protocol, and one participant reported changes in medication/health status during the experiment. Finally, two participants were considered statistical outliers (defined as >2 SD from the average score of participants greater than 50 years of age) on the Montreal Cognitive Assessment (MoCA) (Nasreddine et al., 2005). Data for final analyses were obtained from 86 participants. MoCA scores (Mean ± SD) of the included participants greater than 50 years of age (n = 41) was 27.6 ± 1.7.

2.2. Procedure and data collection

The experimental protocol consisted of three experimental sessions; see also King et al. (2017). The first session was used for screening/familiarization purposes, during which participants were informed about the experiment, completed screening-related questionnaires and assessments (i.e., health history, MRI contraindications, MoCA, etc.), and executed familiarization blocks of practice on the bimanual coordination task (BCT) while positioned supine in a mock MRI scanner (see below for BCT details). The subsequent two sessions consisted of MRI scanning and were completed at the University Hospital of KU Leuven. The first scanning session consisted of a standard scanning protocol, including the acquisition of a high-resolution T1-weighted structural image and ^{1}H-MRS (see below for scan acquisition details). The second scanning session was completed approximately one week following the first and consisted of 9 runs of the BCT while functional MR images were obtained (task-related imaging data not presented here). The Purdue Pegboard task was performed outside the scanner and was administered either in the first or the second testing sessions (immediately before or immediately after the MRI scanning).

2.3. Motor tasks

2.3.1. Purdue pegboard task (PPT)

This task consists of manipulating a maximum number of small pins in two vertical columns with pinholes on a board, within a 30-sec time period (Desrosiers et al., 1995; Tiffin and Asher, 1948, see also Serbruyns et al., 2015). The task was performed with the right hand, left hand, and with both hands simultaneously (in the bimanual condition). Each of the three subtasks was repeated three times. Before starting, the participants were allowed to practice with four pairs of pins. The dependent variable was the average number of pairs inserted during the three bimanual trials.

2.3.2. Bimanual coordination task (BCT)

The BCT and corresponding data have been previously reported (see King et al. (2017) and supplemental materials for a more detailed description of the task). Briefly, participants were positioned supine in the MRS scanner with a non-ferromagnetic device placed on their laps. The device contained two dials (5 cm diameter) to be rotated by the two hands in order to control the movement of a single cursor. The left and right hands controlled movements along the vertical and horizontal axes, respectively. When the left-hand dial was rotated clockwise (CW), the cursor moved up, whereas the cursor moved down when the left-hand dial was rotated counterclockwise (CCW). CW and CCW movements of the right-hand dial resulted in movements to the right and left, respectively. Angular displacements of the dials were registered with non-ferromagnetic high precision optical shaft encoders (HP, 2048 pulses per revolution, sampling frequency of 100 Hz), which were fixed to the movement axes of both dials. Visual information depicting task stimuli and feedback were shown on a LCD projector, visible via a mirror placed in front of the eyes. Four different movement trajectories were included in order to modulate task complexity (see Supplemental Fig. S1). The first

two trajectories required participants to follow a diagonal line on the screen but differed in terms of the slope of the line and thus the relative velocities (i.e., frequency ratios) at which the two hands had to rotate in order to appropriately perform the task. The third condition required the two hands to follow a V- or inverted-V shaped pattern (equal number of trials per block) in which participants had to change the direction or angle of their movement. Last, participants had to abruptly alter directions in a zigzag manner. This Abrupt pattern was either oriented horizontally or vertically (equal number of trials per block). Each BCT session contained eight blocks, with each block consisting of 24 trials (six per movement trajectory) and lasting approximately 6 min. Movement accuracy was the primary measure and reflected the percentage of overlap between the target and the participant's trajectory. Since movement accuracy on all movement trajectory conditions significantly declined with age (King et al., 2017), the dependent variable in this study was taken as the average movement accuracy score collapsed over all BCT blocks and the four movement trajectories.

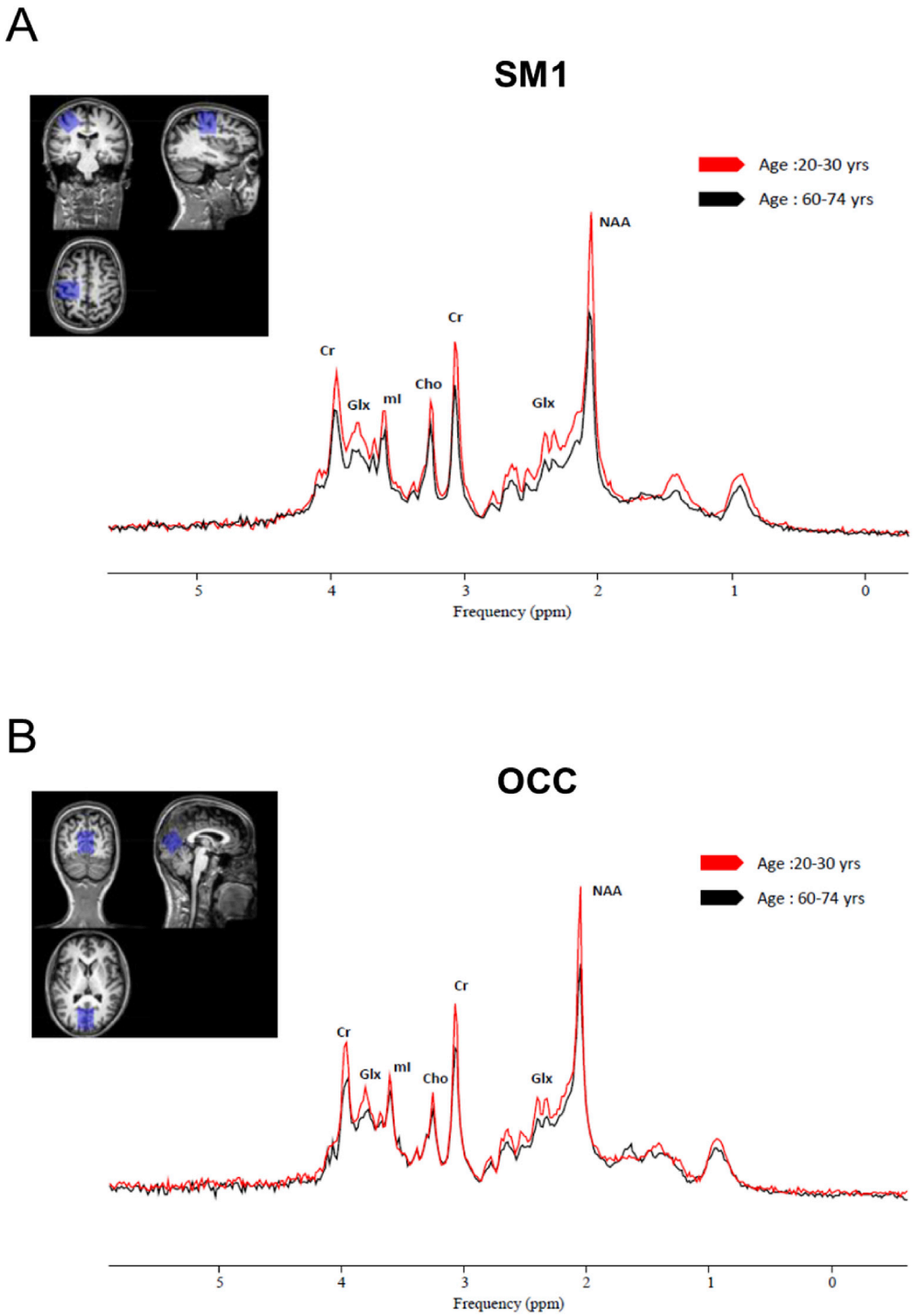


Fig. 1. Primary sensorimotor (SM1) (A) and occipital cortex (OCC) (B) voxels and their corresponding group averaged spectra from the subgroup of younger (20–35 years old cohort, n = 23; red curve) and older (65–75 years old cohort, n = 20; black curve) participants. Group means and variability measures of neurometabolite levels are provided in Supplemental Table S1.

2.4. Brain imaging and ^{1}H-MRS

All scanning sessions were conducted using a Philips 3T Achieva Magnetic Resonance scanner (Philips Healthcare, The Netherlands) with a 32-channel receiver head coil. A high-resolution T1-weighted structural MR image (repetition time (TR) = 9.6 ms, echo time (TE) = 4.6 ms, $0.98 \times 0.98 \times 1.2\,mm^3$ voxels, field of view: $256 \times 256 \times 160$) was used to acquire a 3D magnetization prepared gradient echo (MPRAGE). ^{1}H-MR spectra were acquired in two voxel locations, namely the left sensorimotor cortex (SM1) (Fig. 1A) and occipital cortex (OCC) (Fig. 1B) which are parts of the visuomotor system. MRS data were acquired using a PRESS sequence (TR = 2000 ms, TE = 22 ms, number of averages = 128, spectral bandwidth = 2000 Hz, data size = 1024 points) with excitation water suppression. The voxel size was $1.5 \times 1.5 \times 1.5\,cm^3$ in both the sensorimotor and occipital cortex voxels. The sensorimotor voxel (SM1) was centered over the left hand-knob, parallel to the anterior and posterior axis (Yousry et al., 1997), and was rotated in the coronal and sagittal planes to align with the external surface of the brain (Greenhouse et al., 2016). The occipital voxel (OCC) was centered on the median line, aligned with the cerebellar tentorium in the sagittal plane, and positioned as posteriorly as possible. The unsuppressed water signal was also acquired for absolute metabolite quantification using the same acquisition parameters, except for number of averages = 16. MR spectra were processed using jMRUI v6.0 (Stefan et al., 2009) and the in-house developed software SPID (Poullet et al., 2007). Signal-to-noise ratios (SNR) were determined by jMRUI QUEST in time-domain (maximum of FID/standard deviation of FID tail). Only spectra with linewidths less than 10 Hz or SNR greater than 5 were included for quantification. Spectra were also visually checked to ensure the absence of artefacts. The excluded data were eliminated from further processing. Metabolite signals and corresponding non-suppressed water signals were quantified using peak integration in SPID. Averaged spectra from young (20–35 years) and old (65–75 years) participants are shown in Fig. 1 (for group means and variability measures of neurometabolite levels see Supplemental Table S1). Water-referenced concentrations of NAA, Glx, Cr, Cho, mI and Taurine (Tau) were quantified for each voxel location. Quality control of scanner performance was performed regularly (see also Van Cauter et al., 2013).

The MPRAGE T1-weighted MR images, acquired for the localization and placement of the MRS voxels were segmented with a statistical parametric mapping approach using SPM8 (http://www.fil.ion.ucl.ac.uk/spm/). Voxel registration was performed using custom-made scripts developed in MATLAB (The MathWorks, Natick, Massachusetts, USA) by Dr. Nia Goulden (Bangor University Wales, UK), which can be accessed at http://biu.bangor.ac.uk/projects.php.en (Sanaei Nezhad et al., 2017). Using the T1-weighted MR image and the orientation and location information from the Philips SPAR files, the scripts generate a mask of the voxel location, which is then used to calculate the partial volumes of gray matter (GM), white matter (WM), and cerebrospinal fluid (CSF) percentages within the voxel. The segmented tissue fractions were then used to correct for metabolite concentrations quantified using SPID for differences in CSF content according to Gasparovic et al. (2006). T1 and T2 values used in our study were 1331 ms, 832 ms, and 3817 ms (T1) and 110 ms, 79 ms, and 503 ms (T2) for GM, WM and CSF, respectively. Metabolite relaxation times that were used for calculating the final corrected metabolite concentrations were taken from previous studies (Wansapura et al., 1999; Träber et al., 2004).

2.5. Statistical analysis

Associations between performance measures and brain neurometabolites were examined using regression analyses. Variables of interest were the average numbers of pairs inserted during performance of the bimanual variant of the PPT, average accuracy (collapsed across blocks, trials and conditions) on the BCT and estimated (water-referenced, tissue-corrected) concentrations of NAA, Glx, Cho, Cr, mI, and Tau in the SM1 and OCC regions.

Correlation analyses (Pearson's R) were used to evaluate the bivariate correlation between each neurometabolite and performance as well as age. To adjust for multiple correlation tests, we employed Bonferroni corrections as follows: (1) A corrected value of $p < 0.0042$ (= 0.05/12) was set as significance threshold for correlations between age and concentrations of NAA, Glx, Cho, Cr, mI, and Tau in SM1 and OCC (resulting in 12 correlation tests; i.e., 6 metabolites in 2 voxel locations correlated with age); (2) A corrected value of $p < 0.0021$ (= 0.05/24) was set as significance threshold for correlations between performance on the two coordination tasks and concentrations of NAA, Glx, Cho, Cr, mI, and Tau in SM1 and OCC (resulting in 24 correlation tests; i.e., BCT and PPT performance scores correlated with 6 metabolites in 2 voxel locations).

A Fisher r-to-z transformation was used for comparison between correlations. Note that to control for any potential confounding influence of voxel composition, we conducted secondary correlational analyses nearly identical to that described above but using tissue composition within the voxel or age as covariates (i.e., partial correlations). Results are shown in Supplemental Table S2 (for partial correlations between the tested neurometabolites and age with voxel composition GM and WM as covariates) and Supplemental Table S3 (for partial correlations between neurometabolites and performance with age as a covariate).

Finally, we employed multiple regression analyses to determine the unique variance contributed by specific (putative) neurometabolites to the performance of the PPT and BCT. Putative (candidate) neurometabolites were first selected based on the results of the Pearson's correlation tests and were entered into the regression model if they were significantly correlated with performance and/or age, with exception of Cr which is considered to be a marker of energy metabolism (Soares and Law, 2009). The selected neurometabolites were then removed from the model in a subsequent stepwise step, using the default threshold of $p = 0.01$ to either remove or enter a variable into the model. The same backward stepwise selection process was repeated with no a priori selection of included metabolites (i.e., entering all six neurometabolite in both SM1 and OCC as potential independent variables) in order to ensure that the methodological choice described above did not influence the results. Results of the multiple regression models using the full set of neurometabolites (including Cr) are summarized in Supplemental Table S4 (for PPT) and Supplemental Table S5 (for BCT). All statistical analyses were performed using STATISTICA v13.4 (TIBCO software Inc).

3. Results

3.1. Age-related bimanual performance declines

Our observations revealed significant negative correlations between age and performance on both bimanual tasks, indicating a general decline in coordination abilities with age. Fig. 2A shows the correlation between age and performance scores on the PPT ($r = -0.51$; $p < 0.001$) and Fig. 2B shows the correlation between age and performance scores on the BCT ($r = -0.73$; $p < 0.001$). Finally, the BCT performance scores positively correlated with the performance scores obtained on the PPT ($r = 0.38$; $p < 0.001$). However, the partial correlation between the two performance scores with age inserted as a covariate was not significant (partial-$r = 0.00$, $p > 0.9$), indicating that the two tasks were not related to each other after factoring out the variance explained by age.

3.2. Age-related neurometabolite changes

Plots showing the linear regressions between age and the tissue-corrected concentrations of the six neurometabolites in SM1 and OCC regions are shown in Fig. 3. Bonferroni corrected α-level was set to $p \leq 0.0042$. Significant negative correlations between age and neurometabolite concentrations in the SM1 were found for NAA ($r = -0.43$, $p < 0.001$), Glx ($r = -0.32$, $p = 0.003$), and Cr ($r = -0.33$, $p = 0.002$) (Fig. 3A). Significant negative correlations between age and

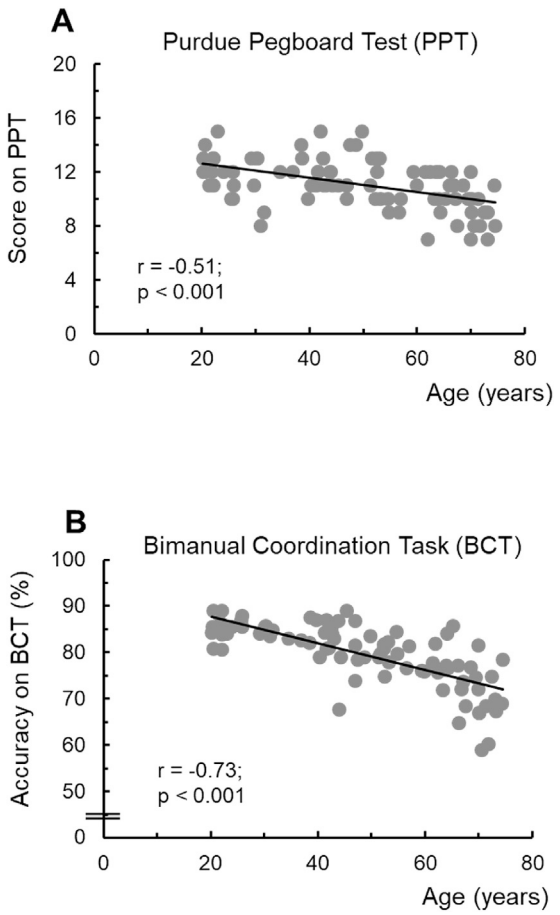


Fig. 2. Linear-regression plots of performance levels by age (n = 86). (A) Performance on the Purdue Pegboard Test (PPT), showing the average number of pairs inserted. (B) Performance on the Bimanual Coordination Task (BCT), showing the accuracy scores collapsed over all BCT sessions and the four movement trajectories.

neurometabolite concentrations in the OCC were found for NAA ($r = -0.43$, $p < 0.001$), Glx ($r = -0.37$, $p < 0.001$), Cr ($r = -0.36$, $p = 0.001$), and Cho ($r = -0.31$, $p = 0.004$) (Fig. 3B). The remaining correlations did not reach statistical significance after correction for multiple comparisons (SM1: Cho, mI, and Tau (all ps ≥ 0.023); OCC: mI, and Tau (both ps ≥ 0.007)). Age-related trajectories were relatively similar across the various metabolites, as a significant difference between the age-related changes in concentration (i.e., correlation coefficients) was only revealed for SM1 NAA ($r = -0.43$) and SM1 Tau ($r = -0.09$); Fisher r-to-z transformation: $z = -2.38$, $p = 0.009$ (otherwise all $|z| \leq 1.56$, $p > 0.05$). Finally, results of partial correlations with SM1 or OCC gray or white mater fractions as covariates revealed a nearly identical pattern of results (see Supplemental Table S2; Fisher r-to-z transformation: all $|z| < 0.3$, $p > 0.4$), suggesting that changes in concentrations with age cannot be explained by age-related changes in voxels' tissue composition. Note, however, that significant changes in voxel tissue composition with age occurred only in the GM of the SM1 voxel ($r = -0.24$, $p = 0.026$); for details, see Supplemental Fig. S2.

3.3. Relationship between MRS metrics and motor performance

3.3.1. Relationship between MRS metrics and motor performance on PPT

Results of the correlation (Pearson) analyses revealed significant positive associations between PPT performance and SM1 levels of NAA ($r = 0.39$, $p < 0.001$), Glx ($r = 0.34$, $p = 0.001$), Cr ($r = 0.42$, $p < 0.001$), and mI ($r = 0.41$, $p < 0.001$) (see Fig. 4A and Supplemental Table S3; Bonferroni-corrected α-level was set to $p \leq 0.0021$). Among these, only the correlation between performance on the PPT and SM1 level of mI was robust to partial correlation with age (partial-$r = 0.34$, $p = 0.003$); see Supplemental Table S3. However, Fisher r–to-z transformations showed no significant differences between non-age adjusted and age-adjusted correlation coefficients (all $|z| \leq 1.21$, $p > 0.1$). In addition, no significant differences between correlation coefficients were found for any of the six metabolites in the two voxel locations (all $|z| \leq 1.28$, $p > 0.1$). Taken together, results of the correlation analyses suggested that performance declines on the PPT could be attributed, primarily, to the proportionately lower concentrations of SM1 NAA, Glx, and mI.

The multiple-regression model including the six neurometabolites showing significant correlations with age and/or performance (i.e., SM1 NAA, SM1 Glx, SM1 mI, OCC NAA, OCC Glx, and OCC Cho) revealed that, collectively, the six selected neurometabolites explained 22.3% of the variance in performance on the PPT. However, none contributed independently (see Table 1). Using the stepwise regression procedure on the same subset of neurometabolites revealed that the SM1 mI ($t(84) = 4.10$, $p < 0.0001$) was shown to be a significant and independent predictor of PPT performance, accounting for 16.7% of the variance (Table 2). A more detailed examination of the results indicated, however, that OCC Cho accounted for 5.4% of the variance in performance. The collective contribution of Glx and NAA in both voxel locations to the performance on the PPT was negligible (explained less than 1% of the variance). Nearly similar observations were obtained when all 12 predictors (i.e., NAA, Glx, Cr, Cho, mI, and Tau in both voxel locations) were entered into the stepwise regression procedure. Note, however, that here SM1 Glx accounted for 3.9% of the variance in performance whereas the remaining nine neurometabolites collectively accounted for 7% of the variance (see Supplemental Table S4).

3.3.2. Relationship between MRS metrics and motor performance on BCT

For the BCT, significant positive associations were observed between the average accuracy scores and SM1 levels of NAA ($r = 0.37$, $p < 0.001$) and Glx ($r = 0.32$, $p = 0.002$), and OCC levels of NAA ($r = 0.33$, $p = 0.002$) (see Fig. 4B). These relationships, however, were not robust to partial correlations with age as a covariate; all partial-$r \leq 0.31$, ps > 0.005 (see Supplemental Table S3). Significant differences between non-age adjusted and age-adjusted correlation coefficients were found for SM1 NAA (non-age adjusted $r = 0.37$ versus age-adjusted partial correlation $r = 0.08$; Fisher r–to-z transformations: $z = 1.95$, $p = 0.026$) and OCC NAA (non-age adjusted $r = 0.33$ versus age-adjusted partial correlation $r = 0.02$; Fisher r-to-z transformation: $z = 2.08$, $p = 0.019$) but not for SM1 Glx (non-age adjusted $r = 0.32$ versus age-adjusted partial correlation $r = 0.14$; Fisher r-to-z transformation: $z = 1.25$, $p > 0.1$). The aforementioned finding suggests that the significant association between MRS metrics and motor performance on the BCT is largely driven by age.

The multiple-regression model including the five neurometabolites showing significant correlations with age and/or performance (i.e., SM1 NAA, SM1 Glx, OCC NAA, OCC Glx, and OCC Cho) revealed that, collectively, the five selected neurometabolites explained 21.2% of the variance in performance on the BCT. However, none contributed independently (see Table 3). Using the stepwise regression procedure on the same subsets of neurometabolites revealed that the SM1 NAA was a significant and independent predictor of BCT ($t(84) = 3.64$, $p = 0.0005$), contributing 13.6% to the variance in performance (Table 4). Further examination of the results indicated that NAA OCC accounted for 6.00% of the variance whereas the collective contribution to the variance of the three remaining neurometabolites (i.e., SM1 Glx, OCC Glx, and OCC Cho) was less than 2%. Similar observations were obtained when all 12 predictors were entered into the stepwise regression procedure (see Supplemental Table S5).

4. Discussion

The main objective of the current study was to correlate

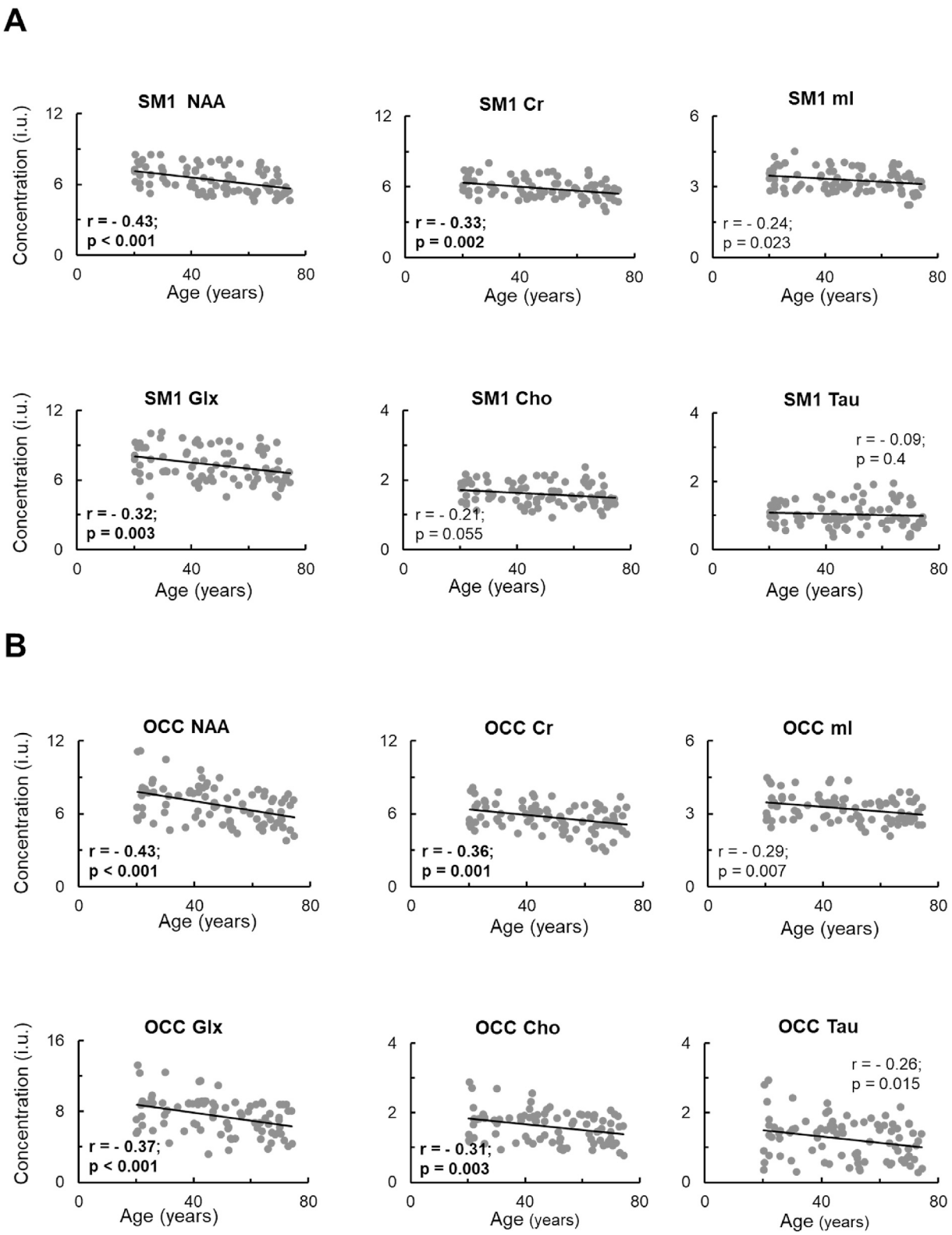


Fig. 3. Linear-regression plots of metabolite levels by age in primary sensorimotor (SM1) (A) and occipital cortex (OCC) (B) voxels. (B). Abbreviations: i.u. = institutional units; N-acetylaspartate; Glx = glutamate-glutamine complex; Cr = creatine + phosphocreatine; Cho = choline; mI = myoinositol; Tau = Taurine. The correlation coefficients were considered significant when p-values were below the Bonferroni corrected threshold at $p < 0.0042$ (= 0.05/12), marginally significant when $p < 0.01$, and not significant when $p \geq 0.01$. Significant correlations are highlighted in **bold text**.

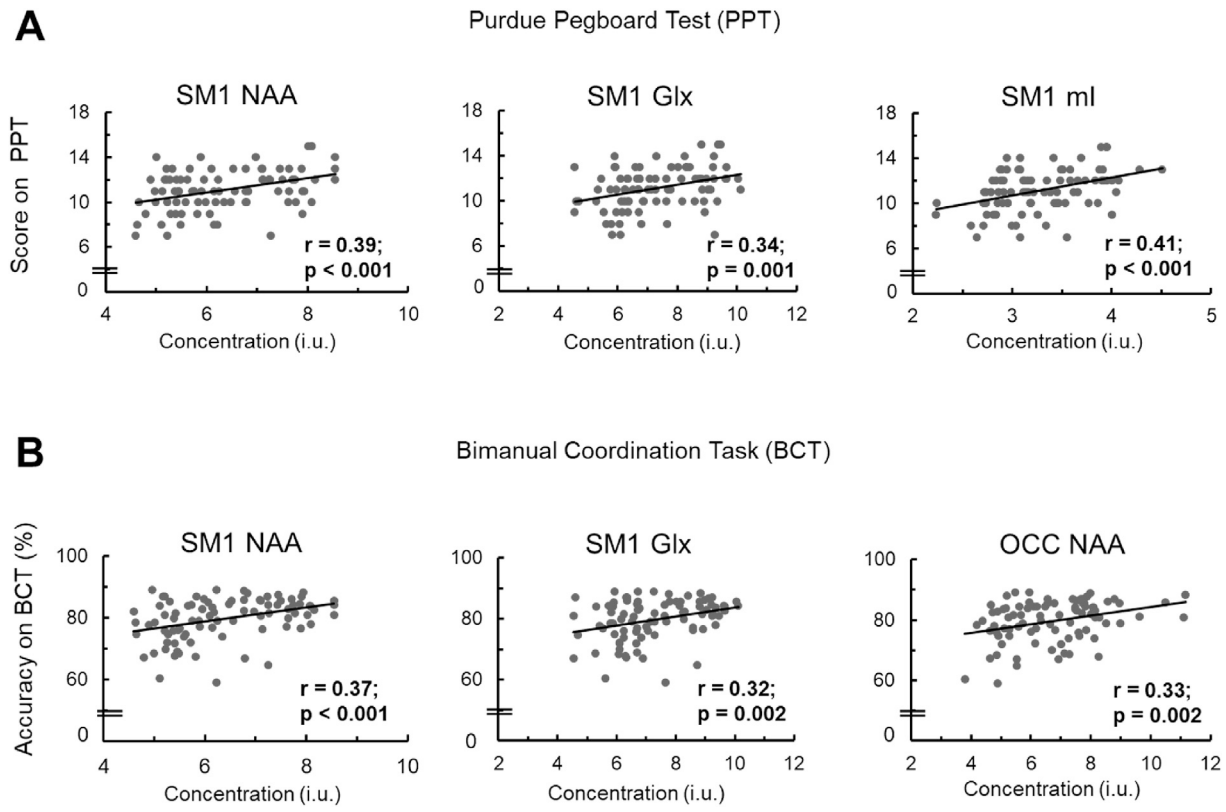


Fig. 4. (A) Linear-regression plots showing the neurometabolite correlates of Purdue Pegboard task (PPT) performance scores (i.e., average number of pairs inserted). Illustrations are shown for SM1 NAA, Glx, and mI. (B) Linear-regression plots showing the neurometabolite correlates of Bimanual Coordination Task (BCT) performance. Illustrations are shown for SM1 NAA and Glx and OCC NAA. See Supplemental Table S3 for correlations with the remaining neurometabolites. Abbreviations: i. u. = institutional units; N-acetylaspartate; Glx = glutamate-glutamine complex; mI = myoinositol; SM1 = sensorimotor voxel positioning; OCC = occipital cortex voxel positioning. The correlation coefficients were considered significant when p-values were below the Bonferroni corrected threshold at $p < 0.0021$ (= 0.05/24).

Table 1
Results of the multiple regression between performance measures on the Purdue Pegboard Task (PPT) and putative (selected) neurometabolite predictors.

R^2	R^2-Adj.	F(6,79)		β (SE)	B (SE)	t(79)	p-value
0.233	0.175	4.008**					
			Intercept		4.29 (1.47)	2.922	0.0046
			SM1 NAA	0.26 (0.32)	0.44 (0.52)	0.835	0.4062
			SM1 Glx	−0.26 (0.31)	−0.33 (0.39)	−0.839	0.4039
			SM1 mI	0.38 (0.19)	1.48 (0.77)	1.936	0.0565
			OCC NAA	0.05 (0.31)	0.06 (0.36)	0.172	0.8641
			OCC Glx	0.09 (0.29)	0.08 (0.25)	0.311	0.7565
			OCC Cho	0.09 (0.31)	0.38 (1.25)	0.301	0.7641

SM1 = primary sensorimotor cortex; OCC = occipital cortex; NAA = N-acetylaspartate; Glx = glutamate-glutamine complex; Cho = choline; mI = myoinositol; B = regression coefficient; β = standardized regression coefficient; SE = standard error; R^2 = Multiple R^2; R^2-Adj = Adjusted R^2; *p < 0.05; ** p < 0.01; *** p < 0.001.

neurometabolite and behavioral changes in a lifespan cohort. Our findings provide novel evidence that neurometabolic changes in the aging left sensorimotor cortex (SM1) are associated with age-related declines in bimanual coordination skills. A first major observation was that (tissue-corrected) levels of multiple neurometabolites in both the left sensorimotor and occipital regions of the healthy human brain decreased significantly with age. A second major observation was that lower NAA levels in the left SM1 corresponded to poorer levels of performance on the BCT, a visuomotor task that has shown associations with brain structural and functional connectivity measures (Fujiyama et al., 2016; King et al., 2017; Solesio-Jofre et al., 2014). Moreover, decreased performance on the Purdue Pegboard task was predicted by lower levels of mI in the SM1. Overall, our findings suggest that age-related alterations of neurochemical levels in SM1 (specifically but not exclusively NAA and mI) could serve as correlates of motor performance across the adult lifespan.

4.1. *Effects of age on neurometabolite levels in SM1 and OCC*

Findings from the current MRS data showed an overall age-related decrease in the concentration of NAA, Glutamate/Glutamine (Glx), and Cr in both voxel locations. These changes could come along with reduced GM and/or WM volume and/or neuronal loss (Ding et al., 2016; Eylers et al., 2016). A significant age-related decline in Cho level was observed only in the OCC voxel, whereas, for the remaining metabolites, only weak and/or moderate trends towards lower levels in older age (mI and Cho in the SM1 voxel and mI and Tau in the OCC voxel) or no age effects at all (SM1 Tau) were found. It should be noted, however, that trends towards declining Cr, Cho, mI, and Tau are not supported by the partially contradicting literature (Chiappelli et al., 2015; Cichocka and Bereś, 2018;

Table 2

(A) Main neurometabolic predictors of motor performance obtained by stepwise regression between behavioral motor measures on the Purdue Pegboard Task (PPT) and the putative (selected) neurometabolite predictors (NAA, Glx, and mI concentrations in the SM1 and NAA, Glx and Cho concentrations in the OCC). The significant and independent predictor (SM1 NAA) is highlighted in **bold text**. **(B)** Summary of the stepwise (backward) regression steps. The removed neurometabolic predictors are sorted from first (OCC NAA) to last (OCC Cho) out in the order of removal.

(A)	R^2	R^2-Adj.	F(1,84)		β (SE)	B (SE)	t(84)	p-value
	0.167	0.157	16.81***					
				Intercept		5.87 (1.30)	4.526	0.0000
				SM1 mI	**0.41 (0.10)**	**1.60 (0.39)**	**4.100**	**0.0001**
(B)				Predictor	R^2	R^2 - Change	F –to enter/remove	p –value
				Combined	0.233			
				OCC NAA	0.233	−0.000	0.029	0.8641
				OCC Glx	0.231	−0.002	0.177	0.6750
				SM1 Glx	0.222	−0.009	0.933	0.3369
				SM1 NAA	0.221	−0.002	0.161	0.6896
				OCC Cho	0.167	−0.054	5.778	0.0185

SM1 = primary sensorimotor cortex; OCC = occipital cortex; Combined = all selected neurometabolites; NAA = N-acetylaspartate; Glx = glutamate-glutamine complex; Cho = choline; mI = myoinositol; B = regression coefficient; β = standardized regression coefficient; SE = standard error; R^2 = Multiple R^2; R^2-Adj = Adjusted R^2; *p < 0.05; ** p < 0.01; *** p < 0.001.

Table 3

Results of the multiple regression between performance measures on the Bimanual Coordination Task (BCT) and putative (selected) neurometabolite predictors.

R^2	R^2-Adj.	F(5,80)		β (SE)	B (SE)	t(80)	p-value
0.212	0.162	4.298**					
			Intercept		59.8 (4.46)	13.42	0.0000
			SM1 NAA	0.34 (0.31)	2.07 (1.88)	1.103	0.2735
			SM1 Glx	−0.05 (0.30)	−0.22 (1.40)	−0.159	0.8744
			OCC NAA	0.60 (0.31)	2.59 (1.33)	1.942	0.0556
			OCC Glx	−0.20 (0.29)	−0.67 (0.94)	−0.709	0.4804
			OCC Cho	−0.17 (0.31)	−2.55 (4.66)	−0.547	0.5861

SM1 = primary sensorimotor cortex; OCC = occipital cortex; NAA = N-acetylaspartate; Glx = glutamate-glutamine complex; Cho = choline; B = regression coefficient; β = standardized regression coefficient; SE = standard error; R^2 = Multiple R^2; R^2-Adj = Adjusted R^2; *p < 0.05; ** p < 0.01; *** p < 0.001.

Table 4

(A) Main neurometabolic predictors of motor performance obtained by stepwise regression between behavioral motor measures on the Bimanual Coordination Task (BCT) and the putative (selected) neurometabolite predictors (NAA and Glx, concentrations in the SM1 and NAA, Glx, and Cho concentrations in the OCC). The significant and independent predictor (SM1 NAA) is highlighted in **bold text**. **(B)** Summary of the stepwise (backward) regression steps. The removed neurometabolic predictors are sorted from first (SM1 Glx) to last (OCC NAA) out in the order of removal.

(A)	R^2	R^2-Adj.	F(1,84)		β (SE)	B (±SE)	t(84)	p-value
	0.136	0.126	13.24***					
				Intercept		65.3 (4.01)	16.28	0.0000
				SM1 NAA	**0.37 (0.10)**	**2.26 (0.62)**	**3.64**	**0.0005**
(B)				Predictor	R^2	R^2 - Change	F –to enter/remove	p-value
				Combined	0.212			
				SM1 Glx	0.211	−0.000	0.025	0.8744
				OCC Cho	0.208	−0.003	0.345	0.5586
				OCC Glx	0.196	−0.012	1.240	0.2688
				OCC NAA	0.136	−0.060	6.193	0.0148

SM1 = primary sensorimotor cortex; OCC = occipital cortex; Combined = all selected neurometabolites; NAA = N-acetylaspartate; Glx = glutamate-glutamine complex; Cho = choline; B = regression coefficient; β = standardized regression coefficient; SE = standard error; R^2 = Multiple R^2; R^2-Adj = Adjusted R^2; *p < 0.05; ** p < 0.01; *** p < 0.001.

Ding et al., 2016; Schmitz et al., 2018 Zahr et al., 2013). It is important to recognize that the effects of normal aging on regional metabolite levels appear to be inconsistent across regions or age groups (Cleeland et al., 2019). For example, Zahr et al. (2013) reported in a similar cohort that levels of total Cr (tCr) in the striatum were lower in older than younger adults whereas levels of tCr in the cerebellum were higher in older than in younger adults. Other metabolites (such as NAA and glutamate-glutamine complex) often showed robust trends across studies (Cleeland et al., 2019). Nevertheless, regional differences in trends (or absence of age-related changes in regional concentration levels) were reported even for these metabolites (Zahr et al., 2013; Ding et al., 2016).

Age-related changes in neurometabolite concentration may be partly caused by region-specific structural neurodegenerative processes, as proposed by Grachev and Apkarian (2001). In our study, significant negative correlations were found between age and NAA, Cr, and Glx levels in both voxel locations, even though the age effect was slightly more pronounced for NAA. This is consistent with previous studies reporting a declining trend of NAA and Glx levels with age across multiple cortical and subcortical regions, including the primary sensorimotor cortex (Kaiser et al., 2005), striatum (Zahr et al., 2013), hippocampus (Harris et al., 2014), and the prefrontal lobe (Ding et al., 2016).

The finding that age-related changes in NAA and Glx concentrations occur in parallel could suggest that changes in brain tissue volume and brain metabolite concentrations with age may be triggered by shared neurodegenerative processes, or vice versa. Similar to NAA, age-dependent decreases of Glx content are expected to occur

predominantly due to loss of neuronal density (e.g., Ding et al., 2016; Eylers et al., 2016). Decreases in neuronal metabolic activity may impair synthesis of glutamate and, therefore, can be considered as another contributing factor to age-related decline in Glx levels. However, determining the exact mechanism responsible for the decrease is difficult since MRS measures reflect both intra- and extracellular Glx levels. It was not within the scope of the present study to explore the underlying mechanisms leading to neurometabolic changes in the aging brain.

4.2. Neurometabolic correlates of motor performance

In line with previous studies, we observed a progressive decline in bimanual performance with age (Boisgontier et al., 2016; Fujiyama et al., 2012, 2016; Heuninckx et al., 2004; King et al., 2017; Serrien et al., 2000; Swinnen et al., 1998). Such declines have been attributed to multiple factors, including loss of GM and WM volume (Boisgontier et al., 2016; Fling and Seidler, 2012; Fling et al., 2011; Koppelmans et al., 2015; Serbruyns et al., 2015), breakdown in the brain's organization of functional networks (King et al., 2017), and/or disruption of structural/functional connectivity between motor and non-motor brain regions (Fujiyama et al., 2016; Levin et al., 2014). The observations from the current study suggest that neurometabolic changes across the lifespan may also be a contributing factor to the observed motor performance declines with increasing age.

Our findings extend previous observations which highlighted the associations between changes in prefrontal or striatal concentrations of NAA or Glx and declines in motor or cognitive functioning in older adults without overt diseases (Nikolaidis et al., 2017; Zahr et al, 2008, 2013). Both NAA and Glx correlated significantly with performance on both bimanual tasks. However, the regression analyses established that, as compared to NAA (for BCT) or mI (for PPT), changes in SM1 Glx levels did not contribute significantly to performance variance. A partial explanation for the overall detrimental effects of SM1 NAA (and mI) but not SM1 Glx concentration declines on performance is that age-related performance declines are triggered primarily by loss of structural integrity of the prefrontal-motor network rather than by age-related differences in integrity of glutamatergic (and GABAergic) systems in SM1. For example, Fujiyama et al. (2016) clearly associated reduced microstructural white matter organization of interhemispheric fiber tracts to poorer bimanual performance. The same study revealed no association between age-related changes in M1-M1 interhemispheric inhibition or facilitation (which are mediated by GABAergic and Glutamatergic signaling, respectively) and performance changes on the bimanual task.

Evidence linking changes in the concentration of other brain neurometabolites (such as NAA) to performance deficits was provided from previous studies on pathological aging (Chiappelli et al., 2015; Kantarci et al., 2002; Tumati et al., 2018; Zanigni et al., 2015) or individuals with brain injuries (Grossman et al., 2015). Importantly, decreases in NAA concentration have previously been linked to reduced microstructural organization of WM in normal aging and in pathological conditions (Bjartmar et al., 2000; Bonneville et al., 2002; Chiappelli et al., 2015; Grossman et al., 2015; Wijtenburg et al., 2013). As such, the present finding on the positive relationship between SM1 NAA levels and bimanual accuracy scores (BCT) suggests that reduced NAA may reflect impaired functional integrity of brain networks that support bimanual control. Recent studies on associations between multiple measures of brain network integrity in cohorts of healthy older adult volunteers as well as patients with neurodegenerative diseases support this contention (Lord et al., 2017; Xiang et al., 2019). First, Xiang et al. (2019) reported a significant positive association between fronto-parietal and central lobe functional connectivity and NAA concentration in the dorsolateral prefrontal cortex (DLPFC) in healthy individuals but not in schizophrenia patients. Second, Lord et al. (2017) showed that NAA levels in the posterior cingulate cortex (PCC) were associated with the level of communication both within the PPC as well as between this region and other brain regions. Finally, Fujiyama et al. (2016) revealed that a decreased ability to regulate the interaction between DLPFC and M1 is significantly correlated with performance on a bimanual task similar to the one we used. Taken together, these findings highlight the potential relevance of NAA as a biochemical marker of overall brain network integrity. Future research should examine the extent by which declines in NAA levels are linked to reduced structural connectivity and disrupted neural network communication in healthy (as well as pathological) aging.

Finally, our findings showed that SM1 mI levels were positively associated with performance on the Purdue Pegboard task (PPT). However, a careful examination of the available literature requires additional considerations since multiple studies have indicated that mI levels slightly increase with age (Chiappelli et al., 2015; Raininko and Mattsson, 2010; Reyngoudt et al., 2012; Zahr et al., 2013). This would suggest a negative association between cortical and/or subcortical levels of mI and performance, a finding that is in contrast to our observations. Importantly, our correlation analyses also revealed that poorer performance on the PPT was associated with lower NAA and Glx levels in the SM1 (Fig. 4). Even though these relationships were not supported by the outcome of the multiple regression model, they appear sensible in view of both current observations and existing literature. Specifically, NAA has been shown to correlate with performance on the BCT whereas Zahr et al. (2013) indicated that age-related declines in striatal Glx correlate with poorer performance on a Grooved Pegboard task (a variant of the PPT). Together, the aforementioned observations suggest that, besides declining mI, lower NAA and Glx may also be considered as neurometabolite correlates of performance declines on the PPT. Moreover, given that SM1 NAA and SM1 Glx levels were positively associated with better performance on both the BCT and PPT, we propose that reduced concentrations of NAA and Glx in the primary sensorimotor cortex may constitute a biomarker of motor dysfunction in aging, irrespective of task characteristics. The role of mI in aging, nonetheless, requires further attention.

5. Conclusions

We have shown that levels of multiple neurometabolites in both SM1 and OCC regions of the healthy human brain decrease significantly with age and that lower NAA levels in the left SM1 are associated with age-related declines in bimanual performance. Given that NAA may reflect neurodegenerative processes related to alterations in WM microstructure, these findings highlight the necessity to make use of multiparametric MR imaging approaches to reveal interactions between brain structure, neurochemicals and behavior. Neurometabolite concentrations in other brain regions are also important to consider because motor functions are orchestrated via interactions between the motor and other brain networks (including subcortical structures). Further studies are necessary to conclude whether the positive association between mI levels and motor performance indeed arise from alterations in structural and functional integrity of SM1.

Disclosure statement

The authors disclose no conflicts of interest.

Acknowledgements

This work was supported by the KU Leuven Special Research Fund (grant C16/15/070), the Research Foundation – Flanders (FWO; G.089818N), the Excellence of Science grant (EOS, 30446199, MEMODYN), and the Francqui Foundation awarded to SPS and coworkers. AW and UH acknowledge financial support by the EC-FP7 MC ITN 'TRANSACT' 2012 (No. 316679) and the KU Leuven program financing 'IMIR' (PF10/017). BRK acknowledges financial support by European Union's Horizon 2020 research and innovation programme under the Marie Skłodowska-Curie grant agreement (No. 703490) and a post-doctoral fellowship from the Research Foundation-Flanders (FWO; No

132635). The authors wish to thank Joren Bosman and Jeroen Buvé for assistance with data processing.

Appendix A. Supplementary data

Supplementary data to this article can be found online at https://doi.org/10.1016/j.neuroimage.2019.116050.

References

Beets, I.A.M., Gooijers, J., Boisgontier, M.P., Pauwels, L., Coxon, J.P., Wittenberg, G., Swinnen, S.P., 2015. Reduced neural differentiation between feedback conditions after bimanual coordination training with and without augmented visual feedback. Cerebr. Cortex 25, 1958–1969.

Ben Salem, D., Walker, P.M., Aho, S., Tavernier, B., Giroud, M., Tzourio, C., Ricolfi, F., Brunotte, F., 2008. Brain flexibility and balance and gait performances mark morphological and metabolic abnormalities in the elderly. J. Clin. Neurosci. 15, 1360–1365.

Bjartmar, C., Kidd, G., Mork, S., Rudick, R., Trapp, B.D., 2000. Neurological disability correlates with spinal cord axonal loss and reduced N-acetyl aspartate in chronic multiple sclerosis patients. Ann. Neurol. 48, 893–901.

Block, W., Karitzky, J., Träber, F., Pohl, C., Keller, E., Mundegar, R.R., Lamerichs, R., Rink, H., Ries, F., Schild, H.H., Jerusalem, F., 1998. Proton magnetic resonance spectroscopy of the primary motor cortex in patients with motor neuron disease: subgroup analysis and follow-up measurements. Arch. Neurol. 55, 931–936.

Boisgontier, M.P., van Ruitenbeek, P., Leunissen, I., Chalavi, S., Sunaert, S., Levin, O., Swinnen, S.P., 2016. Nucleus accumbens and caudate atrophy predicts longer action selection times in young and old adults. Hum. Brain Mapp. 37, 4629–4639.

Bonneville, F., Moriarty, D.M., Li, B.S., Babb, J.S., Grossman, R.I., Gonen, O., 2002. Whole-brain N-acetylaspartate concentration: correlation with T2-weighted lesion volume and expanded disability status scale score in cases of relapsing-remitting multiple sclerosis. AJNR, Am. J. Neuroradiol. 23, 371–375.

Boumezbeur, F., Mason, G.F., de Graaf, R.A., Behar, K.L., Cline, G.W., Shulman, G.I., Rothman, D.L., Petersen, K.F., 2010. Altered brain mitochondrial metabolism in healthy aging as assessed by in vivo magnetic resonance spectroscopy. J. Cereb. Blood Flow Metab. 30, 211–221.

Chen, R., 2004. Interactions between inhibitory and excitatory circuits in the human motor cortex. Exp. Brain Res. 154, 1–10.

Chiappelli, J., Hong, L.E., Wijtenburg, S.A., Du, X., Gaston, F., Kochunov, P., Rowland, L.M., 2015. Alterations in frontal white matter neurochemistry and microstructure in schizophrenia: implications for neuroinflammation. Transl. Psychiatry 5, e548.

Cichocka, M., Bereś, A., 2018. From fetus to older age: a review of brain metabolic changes across the lifespan. Ageing Res. Rev. 46, 60–73.

Cleeland, C., Pipingas, A., Scholey, A., White, D., 2019. Neurochemical changes in the aging brain: a systematic review. Neurosci. Biobehav. Rev. 98, 306–319.

Desrosiers, J., Hébert, R., Bravo, G., Dutil, E., 1995. The Purdue Pegboard Test: normative data for people aged 60 and over. Disabil. Rehabil. 17, 217–224.

Ding, B., Chen, K.M., Ling, H.W., Zhang, H., Chai, W.M., Li, X., Wang, T., 2008. Diffusion tensor imaging correlates with proton magnetic resonance spectroscopy in posterior cingulate region of patients with alzheimer's disease. Dement. Geriatr. Cognit. Disord. 25, 218–225.

Ding, X.Q., Maudsley, A.A., Sabati, M., Sheriff, S., Schmitz, B., Schütze, M., Bronzlik, P., Kahl, K.G., Lanfermann, H., 2016. Physiological neuronal decline in healthy aging human brain - an in vivo study with MRI and short echo-time whole-brain1H MR spectroscopic imaging. Neuroimage 137, 45–51.

Duarte, J.M.N., Lei, H., Mlynárik, V., Gruetter, R., 2012. The neurochemical profile quantified by in vivo 1H NMR spectroscopy. Neuroimage 61, 342–362.

Eylers, V.V., Maudsley, A.A., Bronzlik, P., Dellani, P.R., Lanfermann, H., Ding, X.Q., 2016. Detection of normal aging effects on human brain metabolite concentrations and microstructure with whole-brain MR spectroscopic imaging and quantitative MR imaging. Am. J. Neuroradiol. 37, 447–454.

Fling, B.W., Seidler, R.D., 2012. Fundamental differences in callosal structure, neurophysiologic function, and bimanual control in young and older adults. Cereb.Cortex 22, 2643–2652.

Fling, B.W., Walsh, C.M., Bangert, A.S., Reuter-Lorenz, P.A., Welsh, R.C., Seidler, R.D., 2011. Differential callosal contributions to bimanual control in young and older adults. J. Cogn. Neurosci. 23, 2171–2185.

Fujiyama, H., Hinder, M.R., Schmidt, M.W., Garry, M.I., Summers, J.J., 2012. Age-related differences in corticospinal excitability and inhibition during coordination of upper and lower limbs. Neurobiol. Aging 33, 1481–1484.

Fujiyama, H., Van Soom, J., Rens, G., Gooijers, J., Leunissen, I., Levin, O., Swinnen, S.P., 2016. Age-related changes in frontal network structural and functional connectivity in relation to bimanual movement control. J. Neurosci. 36, 1808–1822.

Gao, F., Edden, R.A.E., Li, M., Puts, N.A.J., Wang, G., Liu, C., Zhao, B., Wang, H., Bai, X., Zhao, C., Wang, X., Barker, P.B., 2013. Magnetic resonance spectroscopy detects an age-related decline in brain GABA levels. Neuroimage 78, 75–82.

Gasparovic, C., Song, T., Devier, D., Bockholt, H.J., Caprihan, A., Mullins, P.G., Posse, S., Jung, R.E., Morrison, L.A., 2006. Use of tissue water as a concentration reference for proton spectroscopic imaging. Magn. Reson. Med. 55, 1219–1226.

Greenhouse, I., Noah, S., Maddock, R.J., Ivry, R.B., 2016. Individual differences in GABA content are reliable but are not uniform across the human cortex. Neuroimage 139, 1–7.

Grachev, I.D., Apkarian, A.V., 2001. Chemical network of the living human brain: evidence of reorganization with aging. Cogn. Brain Res. 11, 185–197.

Grachev, I.D., Swarnkar, A., Szeverenyi, N.M., Ramachandran, T.S., Apkarian, A.V., 2001. Aging alters the multichemical networking profile of the human brain: an in vivo 1H-MRS study of young versus middle-aged subjects. J. Neurochem. 77, 292–303.

Grossman, E.J., Kirov, I.I., Gonen, O., Novikov, D.S., Davitz, M.S., Lui, Y.W., Grossman, R.I., Inglese, M., Fieremans, E., 2015. N-acetyl-aspartate levels correlate with intra-axonal compartment parameters from diffusion MRI. Neuroimage 118, 334–343.

Haga, K.K., Khor, Y.P., Farrall, A., Wardlaw, J.M., 2009. A systematic review of brain metabolite changes, measured with 1H magnetic resonance spectroscopy. healthy aging. Neurobiol. Aging 30, 353–363.

Harris, J.L., Yeh, H.W., Swerdlow, R.H., Choi, I.Y., Lee, P., Brooks, W.M., 2014. High-field proton magnetic resonance spectroscopy reveals metabolic effects of normal brain aging. Neurobiol. Aging 35, 1686–1694.

Heuninckx, S., Debaere, F., Wenderoth, N., Verschueren, S., Swinnen, S.P., 2004. Ipsilateral coordination deficits and central processing requirements associatedwith coordination as a function of aging. J. Gerontol B. Psychol. Sci. Soc. Sci. 59, 225–232.

Hermans, L., Levin, O., Maes, C., van Ruitenbeek, P., Heise, K.F., Edden, R.A.E., Puts, N.A.J., Peeters, R., King, B.R., Meesen, R.L.J., Leunissen, I., Swinnen, S.P., Cuypers, K., 2018a. GABA levels and measures of intracortical and interhemispheric excitability in healthy young and older adults: an MRS-TMS study. Neurobiol. Aging 65, 168–177.

Hermans, L., Leunissen, I., Pauwels, L., Cuypers, K., Peeters, R., Puts, N.A.J., Edden, R.A.E., Swinnen, S.P., 2018b. Brain gaba levels are associated with inhibitory control deficits in older adults. J. Neurosci. 38, 7844–7851.

Kaiser, L.G., Schuff, N., Cashdollar, N., Weiner, M.W., 2005. Scyllo-inositol in normal aging human brain: 1H magnetic resonance spectroscopy study at 4 Tesla. NMR Biomed. 18, 51–55.

Kalra, S., Tai, P., Genge, A., Arnold, D.L., 2006. Rapid improvement in cortical neuronal integrity in amyotrophic lateral sclerosis detected by proton magnetic resonance spectroscopic imaging. J. Neurol. 253, 1060–1063.

Kantarci, K., Smith, G.E., Ivnik, R.J., Petersen, R.C., Boeve, B.F., Knopman, D.S., Tangalos, E.G., Jack Jr., C.R., 2002. 1H magnetic resonance spectroscopy, cognitive function, and apolipoprotein e genotype in normal aging, mild cognitive impairment and Alzheimer's disease. J. Int. Neuropsychol. Soc. 8, 934–942.

Kantarci, K., Weigand, S.D., Petersen, R.C., Boeve, B.F., Knopman, D.S., Gunter, J., Reyes, D., Shiung, M., O'Brien, P.C., Smith, G.E., Ivnik, R.J., Tangalos, E.G., Jack Jr., C.R., 2007. Longitudinal 1H MRS changes in mild cognitive impairment and Alzheimer's disease. Neurobiol. Aging 28, 1330–1339.

King, B.R., van Ruitenbeek, P., Leunissen, I., Cuypers, K., Heise, K.-F., Santos Monteiro, T., Hermans, L., Levin, O., Albouy, G., Mantini, D., Swinnen, S.P., 2017. Age-related declines in motor performance are associated with decreased segregation of large-scale resting state brain networks. Cerebr. Cortex 28, 4390–4402.

Koppelmans, V., Hirsiger, S., Mérillat, S., Jäncke, L., Seidler, R.D., 2015. Cerebellar gray and white matter volume and their relation with age and manual motor performance in healthy older adults. Hum. Brain Mapp. 36, 2352–2363.

Levin, O., Fujiyama, H., Boisgontier, M.P., Swinnen, S.P., Summers, J.J., 2014. Aging and motor inhibition: a converging perspective provided by brain stimulation and imaging approaches. Neurosci. Biobehav. Rev. 43, 100–117.

Liuzzi, G., Horniss, V., Hoppe, J., Heise, K., Zimerman, M., Gerloff, C., Hummel, F.C., 2010. Distinct temporospatial interhemispheric interactions in the human primary and premotor cortex during movement preparation. Cerebr. Cortex 20, 1323–1331.

Lord, A.R., Li, M., Demenescu, L.R., van den Meer, J., Borchardt, V., Krause, A., Heinze, H.J., Breakspear, M., Walter, M.1., 2017. Richness in functional connectivity depends on the neuronal integrity within the posterior cingulate cortex. Front. Neurosci. 11, 184.

Maes, C., Hermans, L., Pauwels, L., Chalavi, S., Leunissen, I., Levin, O., Cuypers, K., Peeters, R., Sunaert, S., Mantini, D., Puts, N.A.J., Edden, R.A.E., Swinnen, S.P., 2017. Age-related differences in GABA levels are driven by bulk tissue changes. Hum. Brain Mapp. (ahead of print); see https://doi.org/10.1002/hbm.24201.

Nasreddine, Z.S., Phillips, N.A., Bédirian, V., Charbonneau, S., Whitehead, V., Collin, I., Cummings, J.L., Chertkow, H., 2005. The Montreal Cognitive Assessment, MoCA: a brief screening tool for mild cognitive impairment. J. Am. Geriatr. Soc. 53, 695–699.

Nikolaidis, A., Baniqued, P.L., Kranz, M.B., Scavuzzo, C.J., Barbey, A.K., Kramer, A.F., Larsen, R.J., 2017. Multivariate associations of fluid intelligence and NAA. Cerebr. Cortex 27, 2607–2616.

Oldfield, R.C., 1971. The assessment and analysis of handedness: the Edinburgh inventory. Neuropsychologia 9, 97–113.

Perez, M.A., Cohen, L.G., 2008. Mechanisms underlying functional changes in the primary motor cortex ipsilateral to an active hand. J. Neurosci. 28, 5631–5640.

Porges, E.C., Woods, A.J., Edden, R.A.E., Puts, N.A.J., Harris, A.D., Chen, H., Garcia, A.M., Seider, T.R., Lamb, D.G., Williamson, J.B., Cohen, R.A., 2017. Frontal gamma-aminobutyric acid concentrations are associated with cognitive performance in older adults. Biol Psychiatry Cogn Neurosci Neuroimaging 2, 38–44.

Poullet, J., Sima, D.M., Simonetti, A.W., De Neuter, B., Vanhamme, L., Lemmerling, P., Van Huffel, S., Neuter, B., Vanhamme, L., 2007. An automated quantitation of short echo time MRS spectra in an open source software environment: AQSES. NMR Biomed. 20, 493–504.

Raininko, R., Mattsson, P., 2010. Metabolite concentrations in supraventricular white matter from teenage to early old age: a short echo time ^{1}H magnetic resonance spectroscopy (MRS) study. Acta Radiol. 51, 309–315.

Reyngoudt, H., Claeys, T., Vlerick, L., Verleden, S., Acou, M., Deblaere, K., De Deene, Y., Audenaert, K., Goethals, I., Achten, E., 2012. Age-related differences in metabolites in the posterior cingulate cortex and hippocampus of normal ageing brain: a 1H-MRS study. Eur. J. Radiol. 81, e223–e231.

Sanaei Nezhad, F., Anton, A., Parkes, L.M., Deakin, B., Williams, S.R., 2017. Quantification of glutathione in the human brain by MR spectroscopy at 3 Tesla: comparison of PRESS and MEGA-PRESS. Magn. Reson. Med. 78, 1257–1266.

Santos Monteiro, T., Beets, I.A.M., Boisgontier, M.P., Gooijers, J., Pauwels, L., Chalavi, S., King, B., Albouy, G., Swinnen, S.P., 2017. Relative cortico-subcortical shift in brain activity but preserved training-induced neural modulation in older adults during bimanual motor learning. Neurobiol. Aging 58, 54–67.

Schmitz, B., Wang, X., Barker, P.B., Pilatus, U., Bronzlik, P., Dadak, M., Kahl, K.G., Lanfermann, H., Ding, X.Q., 2018. Effects of aging on the human brain: a proton and phosphorus MR spectroscopy study at 3T. J. Neuroimaging 28, 416–421.

Serbruyns, L., Leunissen, I., Huysmans, T., Cuypers, K., Meesen, R.L., van Ruitenbeek, P., Sijbers, J., Swinnen, S.P., 2015. Subcortical volumetric changes across the adult lifespan: subregional thalamic atrophy accounts for age-related sensorimotor performance declines. Cortex 65, 128–138.

Serrien, D.J., Swinnen, S.P., Stelmach, G.E., 2000. Age-related deterioration of coordinated interlimb behavior. J. Gerontol. B. Psychol. Sci. Soc. Sci. 55B, 295–303.

Sisti, H.M., Geurts, M., Clerckx, R., Gooijers, J., Coxon, J.P., Heitger, M.H., Caeyenberghs, K., Beets, I.A.M., Serbruyns, L., Swinnen, S.P., 2011. Testing multiple coordination constraints with a novel bimanual visuomotor task. PLoS One 6, e23619.

Soares, D.P., Law, M., 2009. Magnetic resonance spectroscopy of the brain: review of metabolites and clinical applications. Clin. Radiol. 64, 12–21.

Solesio-Jofre, E., Serbruyns, L., Woolley, D.G., Mantini, D., Beets, I.A.M., Swinnen, S.P., 2014. Aging effects on the resting state motor network and interlimb coordination. Hum. Brain Mapp. 35, 3945–3961.

Stefan, D., Cesare, F., Di, Andrasescu, A., Popa, E., Lazariev, A., Vescovo, E., Strbak, O., Williams, S., Starcuk, Z., Cabanas, M., Van Ormondt, D., Graveron-Demilly, D., 2009. Quantitation of magnetic resonance spectroscopy signals: the jMRUI software package. Meas. Sci. Technol. 20, 104035. https://doi.org/10.1088/0957-0233/20/10/104035.

Swinnen, S.P., Verschueren, S., Bogaerts, H., Dounskaia, N., Lee, T., Stelmach, G., Serrien, D., 1998. Age-related deficits in motor learning and differences in feedback processing during the production of a bimanual coordination pattern. Cogn. Neuropsychol. 15, 439–466.

Tiffin, J., Asher, E.J., 1948. The Purdue pegboard; norms and studies of reliability and validity. J. Appl. Psychol. 32, 234–247.

Träber, F., Block, W., Lamerichs, R., Gieseke, J., Schild, H.H., 2004. 1H Metabolite relaxation times at 3.0 Tesla: measurements of T1 and T2 values in normal brain and determination of regional differences in transverse relaxation. J. Magn. Reson. Imaging 19, 537–545.

Tumati, S., Opmeer, E.M., Marsman, J.C., Martens, S., Reesink, F.E., De Deyn, P.P., Aleman, A., 2018. Lower choline and myo-inositol in temporo-parietal cortex is associated with apathy in amnestic MCI. Front. Aging Neurosci. 10, 106.

Valenzuela, M.J., Sachdev, P.S., Wen, W., Shnier, R., Brodaty, H., Gillies, D., 2000. Dual voxel proton magnetic resonance spectroscopy in the healthy elderly: subcortical frontal axonal n-acetylaspartate levels are correlated with fluid cognitive abilities independent of structural brain changes. Neuroimage 12, 747–756.

Van Cauter, S., Sima, D.M., Luts, J., ter Beek, L., Ribbens, A., Peeters, R.R., Osorio Garcia, M.,I., Li, Y., Sunaert, S., Van Gool, S.W., Van Huffel, S., Himmelreich, U., 2013. Reproducibility of rapid short echo time CSI at 3 tesla for clinical applications. J. Magn. Reson. Imaging 37, 445–456.

Wansapura, J.P., Holland, S.K., Dunn, R.S., Ball Jr., W.S., 1999. NMR relaxation times in the human brain at 3.0 tesla. J. Magn. Reson. Imaging 9, 531–538.

Weerasekera, A., Sima, D., Dresselaers, T., Van Huffel, S., Van Damme, P., Himmelreich, U., 2018. Noninvasive assessment of disease progression and neuroprotective effects of dietary coconut oil supplementation in the SOD1G93A mouse model:1H-magnetic resonance spectroscopic study. Neuroimage: Clinic 20, 1092–1105.

Wijtenburg, S.A., McGuire, S.A., Rowland, L.M., Sherman, P.M., Lancaster, J.L., Tate, D.F., Hardies, L.J., Patel, B., Glahn, D.C., Hong, L.E., Fox, P.T., Kochunov, P., 2013. Relationship between fractional anisotropy of cerebral white matter and metabolite concentrations measured using (1)H magnetic resonance spectroscopy in healthy adults. Neuroimage 66, 161–168.

Xiang, Q., Xu, J., Wang, Y., Chen, T., Wang, J., Zhuo, K., Guo, X., Zeljic, K., Li, W., Sun, Y., Wang, Z., Li, Y., Liu, D., 2019. Modular functional-metabolic coupling alterations of frontoparietal network in schizophrenia patients. Front. Neurosci. 13, 40.

Yousry, T.A., Schmid, U.D., Alkadhi, H., Schmidt, D., Peraud, A., Buettner, A., Winkler, P., 1997. Localization of the motor hand area to a knob on the precentral gyrus. A new landmark. Brain 120, 141–157.

Zahr, N.M., Mayer, D., Pfefferbaum, A., Sullivan, E.V., 2008. Low striatal glutamate levels underlie cognitive decline in the elderly: evidence from in vivo molecular spectroscopy. Cerebr. Cortex 8, 2241–2250.

Zahr, N.M., Mayer, D., Rohlfing, T., Chanraud, S., Gu, M., Sullivan, E.V., Pfefferbaum, A., 2013. In vivo glutamate measured with magnetic resonance spectroscopy: behavioral correlates in aging. Neurobiol. Aging 34, 1265–1276.

Zanigni, S., Testa, C., Calandra-Buonaura, G., Sambati, L., Guarino, M., Gabellini, A., Evangelisti, S., Cortelli, P., Lodi, R., Tonon, C., 2015. The contribution of cerebellar proton magnetic resonance spectroscopy in the differential diagnosis among parkinsonian syndromes. Park. Relat. Disord. 21, 929–937.